

Nonlinear coupling between magnetar QPOs

P. PNIGOURAS¹ AND S. K. LANDER²

¹*Departamento de Física Aplicada, Universidad de Alicante, Campus de San Vicente del Raspeig, Alicante E-03690, Spain*

²*School of Engineering, Mathematics and Physics, University of East Anglia, Norwich NR4 7TJ, U.K.*

ABSTRACT

The quasi-periodic oscillations (QPOs) observed in the tails of magnetar giant γ -ray flares have long been interpreted as normal oscillation modes of these stars. However, most studies modelling QPOs have neglected some key features in the analyses of the signals, namely that QPOs appear to be detectable only intermittently and exhibit drifts in their frequencies. These are typical characteristics of nonlinear mode coupling, where, at leading order, the modes couple and evolve collectively as triplets. Using a representative triplet of modes we solve the system's nonlinear equations of motion analytically and argue that the coupling is likely axial-axial-polar in nature, with the observed intermittence and frequency drifts providing a way to infer details of the magnetar's internal magnetic-field geometry.

1. INTRODUCTION

Two decades ago, *quasi-periodic oscillations* (QPOs) were discovered (Israel et al. 2005; Strohmayer & Watts 2005) in the aftermath of giant γ -ray flares from two different *magnetars*, neutron stars (NSs) with very strong magnetic fields $B \sim 10^{14} - 10^{15}$ G characterised by their high-energy outburst activity. These QPOs, in the frequency range of tens to thousands of Hz, seem to represent the first detections of oscillation modes of isolated NSs, and so should encode valuable information about their interior physics, including the critically important NS equation of state (Steiner & Watts 2009), for which there is substantial uncertainty at high densities.

Although the lower-frequency QPOs had the expected properties of elastic shear modes of the NS crust, it quickly became clear that the problem was far more complex. The crust and core are threaded by a strong magnetic field that couples their dynamics, but whose broad structure is not well-understood; this introduces an unwanted degree of ambiguity in the interpretation of observed QPOs as certain modes of the star. Particularly concerning is the possibility that the core admits a continuum of local oscillation frequencies rather than global oscillation modes, as this continuum would tend to drain energy from typical crustal modes (Levin 2007; van Hoven & Levin 2012), although the inclusion of neutron superfluidity helps to resolve this problem (Gabler et al. 2013; Passamonti & Lander 2013, 2014).

Alongside modelling challenges, there have also been various re-analyses of the original data, resulting in conflicting conclusions about how significant and long-lived the different QPOs are (Hambaryan et al. 2011; Pompe et al. 2018; Miller et al. 2019). Although a few additional individual QPOs have been detected from various magnetars (e.g., Castro-Tirado et al. 2021, Roberts et al. 2023), these are no substitute for one new set of high-

quality data that reveals multiple QPOs, and modelling has reached an impasse of simply waiting passively for the next giant flare.

Almost all work on modelling QPOs has focussed on matching numbers: tuning the parameters of a magnetar model so that its oscillation-mode frequencies agree with observed QPOs. Unfortunately, the theoretically-predicted modes are sufficiently densely spaced in frequency that comparison with observations does not place robust constraints on the magnetar's underlying physics. Furthermore, this body of work ignores a major feature of the observations: the QPOs do not behave as if they were all excited at once and then simply decay, like the ringing of a bell. Instead, over hundreds of seconds following the giant flare, QPOs appear and disappear, suggesting some process of decay and re-excitation.

In this Letter, we propose that these features are due to *nonlinear couplings* between different modes. Modelling the couplings would not only help understand the full oscillation tails rather than just single modes, but could also lead to new insight about the physical origin of these modes.

2. REVISITING THE QPOS

To study magnetar mode coupling, we need to identify potential candidate QPOs that could be exhibiting this behaviour. We will look for QPOs following the giant flares of SGR 1806-20 and 1900+14 (hereafter SGR 1806 and SGR 1900) that were detected for more than just a very short segment, and preferably which are common to both magnetars and have been corroborated by more than one study. For SGR 1806, these criteria lead us to select the QPOs at 18, 26, 30, 93, and 150 Hz; there are also a few intriguing QPOs in the kHz range (Israel et al. 2005; Strohmayer & Watts 2006). A subsequent search for QPOs from the far more frequent smaller bursts by Huppenkothen et al. (2014) revealed an additional QPO

at 57 Hz. For SGR 1900, the original data is of lower quality, but the analysis of Strohmayer & Watts (2005) nonetheless yielded QPOs at 28, 53, 84, and 155 Hz.

Since mode coupling is known to cause *frequency drift* (see Section 5), we assume that QPOs of similar frequency represent the same underlying mode; i.e., for SGR 1806, we regard the strong 92.5 Hz and weak 95 Hz QPOs of Israel et al. (2005), and the 90-Hz QPO of Strohmayer & Watts (2006) as the same mode; likewise for the 30-Hz (Israel et al. 2005) and 26-Hz (Watts & Strohmayer 2006) QPOs. This leaves us with four modes observed from both magnetars, with frequencies $\sim 28, 55, 88, 150$ Hz. We will disregard the ~ 150 -Hz mode, partly because it is a very broad peak, and partly because it is closer to the frequency range at which the core continuum of frequencies may affect results.

Our ansatz is that each of the above QPOs represents an oscillation mode of the star of *magneto-elastic* character. To identify candidate physical modes, we use the fitting formulae from Gabler et al. (2016, Equation 20). For the modes to have such a character and not be damped into the continuum, it is required that $10^{14} \text{ G} \lesssim B \lesssim 5 \times 10^{15} \text{ G}$. We can also exclude any oscillations with non-constant phase, whose eigenfunction does not reach the stellar surface, from our modelling.

Satisfying the above, the only plausible triplet involves three of the ‘ ${}^l U_n$ modes’ of Gabler et al. (2016), namely

$${}^2 U_2, {}^6 U_2, {}^6 U_4. \quad (1)$$

Varying the field strength so that the frequencies best match observations, we infer $B = 8.6 \times 10^{14} \text{ G}$ for SGR 1806, which gives triplet mode frequencies of

$$29.8, 56.2, 92.3 \text{ Hz}, \quad (2)$$

and $B = 7.2 \times 10^{14} \text{ G}$ for SGR 1900, yielding

$$27.3, 53.7, 84.0 \text{ Hz}. \quad (3)$$

These values of B are in very good agreement with those inferred from spindown measurements: $7 \times 10^{14} \text{ G}$ for SGR 1900 (Mereghetti et al. 2006) and $8 \times 10^{14} \text{ G}$ for SGR 1806 (Kouveliotou et al. 1998; Younes et al. 2017). Note that the latter is often reported to have a substantially stronger field, $2 \times 10^{15} \text{ G}$, but this value was inferred during a period of enhanced spindown around the time of the giant flare (Palmer et al. 2005) – likely due to an extended corona, making the dipole-spindown formula unreliable.

3. NONLINEAR MODE-COUPLING THEORY

Nonlinear mode coupling is a result of the nonlinear interaction among the oscillation modes of a system. Ever since the work of Dziembowski (1982), this mechanism has been considerably studied in the context of astrophysics, mainly to explain the phenomenology of some variable stars (e.g., Wu & Goldreich 2001), to

study the saturation of neutron star instabilities (Schenk et al. 2001; Arras et al. 2003; Pnigouras & Kokkotas 2015, 2016), and to model the effects of nonlinear tides in binary systems (Weinberg et al. 2012, 2013).

The most basic system is that of three modes, which couple to each other at second order (see e.g. Nayfeh & Mook 1979). In the absence of dissipation, the equations of motion for this system may be written in terms of the mode amplitudes Q_α :

$$\dot{Q}_\alpha = i\omega_\alpha \kappa Q_\beta Q_\gamma e^{-i\Delta\omega t}, \quad (4a)$$

$$\dot{Q}_\beta = i\omega_\beta \kappa Q_\gamma^* Q_\alpha e^{i\Delta\omega t}, \quad (4b)$$

$$\dot{Q}_\gamma = i\omega_\gamma \kappa Q_\alpha Q_\beta^* e^{i\Delta\omega t}, \quad (4c)$$

where ω_α is the mode frequency, $\Delta\omega = \omega_\alpha - \omega_\beta - \omega_\gamma$ is the *detuning parameter* and κ is the mode *coupling coefficient*, defined as an overlap integral among the eigenfunctions ξ_α^i of the three modes [for an explicit expression of κ see, e.g., Schenk et al. (2001) or Dziembowski (1982)]. The mode amplitudes Q_α are defined by the decomposition of a generic perturbation ξ^i in terms of the modes as

$$\xi^i(x^i, t) = \sum_\alpha Q_\alpha(t) \xi_\alpha^i(x^i) e^{i\omega_\alpha t} \quad (5)$$

(note that Q_α does not contain the mode phase).

In spherical, i.e. non-rotating and unmagnetised, stars, each mode can be identified by a single spherical harmonic $Y_l^m(\theta, \phi)$ in a vector spherical harmonic decomposition, namely

$$\xi^i = \frac{W}{r} Y_l^m \nabla^i r + V \nabla^i Y_l^m - iU \epsilon^{ijk} \nabla_j Y_l^m \nabla_k r. \quad (6)$$

Each mode is characterised by a multipole degree l , an azimuthal order m , and its overtone n , denoting the number of nodes in the mode’s radial profile, described by the functions $W(r)$, $V(r)$ and $U(r)$.¹ According to the standard mode classification, we have *polar* modes, in which $U = 0$, and *axial* modes, in which $W = V = 0$.

One may then show that

$$\kappa \propto \iint Y_\alpha^* Y_\beta Y_\gamma \sin \theta d\theta d\phi, \quad (7)$$

with $Y_\alpha \equiv Y_{l_\alpha}^{m_\alpha}$. This is a known integral (e.g., Sakurai & Napolitano 2011), which implies that $\kappa \neq 0$ if

$$m_\alpha = m_\beta + m_\gamma \quad (8)$$

and

$$l_a = l_b + l_c - 2\lambda, \quad (9)$$

where $l_a \geq l_b \geq l_c$ and $\lambda = 0, 1, \dots, \lambda_{\max} \leq l_c/2$, with the indices a, b, c taking the values α, β, γ , so that the

¹ The function U here is not to be confused with the ${}^l U_n$ modes of the Gabler et al. (2016) classification (see Section 2).

mode a has the largest degree and the mode c has the lowest. Equations (8) and (9) constitute the *selection rules* which the coupled mode triplet has to satisfy and restrict the possible couplings.

Finally, the equations of motion (4) imply that, among the many possible couplings, the triplets that ultimately affect the system's dynamics the most are those which satisfy the *nonlinear resonance condition*

$$\Delta\omega = \omega_\alpha - \omega_\beta - \omega_\gamma \simeq 0. \quad (10)$$

4. MODELLING THE BEST TRIPLET

The magneto-elastic modes of Gabler et al. (2016) depend on the magnetic-field structure within the star, with nodes and maxima following the magnetic field lines. Thus, their indices n and l [see Equation (1)] do not have the same meaning as above. An accurate description of such a mode would therefore require an infinite sum of Y_l^m components in a vector spherical harmonic decomposition. This would present severe difficulties in a mode-coupling calculation, due to the various multipolar contributions from each mode entering the coupling coefficient (7). However, aiming for quantitatively accurate mode amplitudes in a calculation that is otherwise necessarily qualitative would be somewhat pointless. Instead, we argue that it is the similarity of the mode eigenfunctions involved in the nonlinear coupling that matters most, effectively establishing how good the overlap among them is and, hence, how strongly they are coupled. With this in mind, we will assume that the coupling of three magnetic lU_n modes is comparable to the coupling of three modes with eigenfunctions of the form of Equation (6) with the same l , n , and therefore proceed by representing each relevant mode from Gabler et al. (2016) as

$$\xi_\alpha^\phi(r, \theta) = C \sin \left[\frac{(2n+1)\pi}{2} \frac{r}{R_*} \right] \frac{\partial_\theta Y_l^0}{\sin \theta}, \quad (11)$$

where R_* is the stellar radius and C is a constant determined by the chosen normalisation. In the above we have adopted the form of an axisymmetric ($m=0$) axial mode, in accordance with Gabler et al. (2016), and have also assumed that the mode's radial dependence is sinusoidal (see e.g. Lee 2008), with the requisite number of nodes n , and non-zero at the surface.

Like almost all other calculations of magnetar QPOs (e.g., Samuelsson & Andersson 2007, Sotani et al. 2007, Cerdá-Durán et al. 2009), the work of Gabler et al. (2016) assumes axial oscillations, since these are more readily excited: they do not involve a radial displacement, which is inhibited by the composition-gradient stratification of the star (Duncan 1998). We therefore begin with the result of Schenk et al. (2001), who calculated the coupling coefficient for a triplet consisting of two axial modes β, γ , and a third mode α whose Eulerian density perturbation $\delta\rho$ vanishes:

$$\kappa_{\alpha\beta\gamma} = \frac{1}{2} \int p(\Gamma_1 - \Gamma) \nabla_k \xi_\alpha^{k*} \nabla_i \xi_\beta^j \nabla_j \xi_\gamma^i dV, \quad (12)$$

with $\Gamma = d \ln p / d \ln \rho$ and $\Gamma_1 = (\partial \ln p / \partial \ln \rho)_{x_p}$, where p is the pressure and ρ is the density. The *adiabatic exponent* Γ_1 differs from the background index Γ if the chemical composition (here denoted by the proton fraction x_p) changes throughout the star.

Since the divergence of an axial mode is zero, Equation (12) shows that there is no coupling between a triplet of axial modes. Thus, mode α must have a polar component. It may still have a leading-order axial piece however; for instance, as is known from stellar perturbation theory, rotation introduces polar corrections to axial modes, and vice versa (e.g., Unno et al. 1989). Therefore, only the polar piece of mode α contributes to $\nabla_i \xi_\alpha^i$. We will regard this divergence as a parameter to adjust; from Equation (6) we have $\nabla_i \xi_\alpha^i = f_\alpha Y_\alpha$, where

$$f_\alpha = \frac{\zeta}{r^2} [\partial_r(rW_\alpha) - l_\alpha(l_\alpha + 1)V_\alpha], \quad (13)$$

with the small parameter ζ quantifying the relative amplitude of the polar piece to the axial piece of the mode.

There are various possible mechanisms for axial-polar mixing, but perhaps the most compelling is related to the magnetic field geometry. The purely poloidal background magnetic fields employed in Gabler et al. (2016) and most other magnetar mode modelling are dynamically unstable (Markey & Tayler 1973; Wright 1973), meaning that only a linked poloidal-toroidal geometry is realistic. Such a field geometry leads to axial modes mixing with polar modes in a manner proportional to the relative strength of toroidal to poloidal field (Colaiuda & Kokkotas 2012). We will therefore regard ζ as a measure of the strength of this toroidal component.

Using Equation (6), the axial-axial-polar coupling coefficient (12) admits the form

$$\begin{aligned} \kappa_{\alpha\beta\gamma} = & -\frac{1}{4} \iint Y_\alpha^* Y_\beta Y_\gamma \sin \theta d\theta d\phi \int p(\Gamma_1 - \Gamma) \left\{ f_\alpha (r g_\beta \partial_r g_\gamma + r \partial_r g_\beta g_\gamma) (-\Lambda_\alpha + \Lambda_\beta + \Lambda_\gamma) \right. \\ & \left. + f_\alpha g_\beta g_\gamma \left[\frac{(\Lambda_\alpha + \Lambda_\beta + \Lambda_\gamma)^2}{2} - (\Lambda_\alpha^2 + \Lambda_\beta^2 + \Lambda_\gamma^2) + 3(-\Lambda_\alpha + \Lambda_\beta + \Lambda_\gamma) \right] \right\} r^2 dr, \quad (14) \end{aligned}$$

where $\Lambda = l(l+1)$ and $g = U/r^2$. For the evaluation of the functions W , V , and U , we will assume that the polar components ξ^r and ξ^θ of mode α take on the same radial dependence as the axial component ξ^ϕ , according to the ansatz (11).

We also define the mode energy as $E_\alpha = 2I_\alpha \omega_\alpha^2 |Q_\alpha|^2$, where

$$I = \int \xi^{i*} \xi_i \rho dV \quad (15)$$

(see e.g. Schenk et al. 2001). The modes will be normalised by fixing their energy to unit amplitude, i.e., $2I_\alpha \omega_\alpha^2 = Mc^2$, with M being the mass of the star and c being the speed of light. Hence, the mode amplitude is simply related to the mode energy through $E_\alpha = |Q_\alpha|^2 Mc^2$.

The same normalisation has been tacitly assumed for the coupling coefficient κ in the derivation of Equations (4); κ is calculated in units of the chosen energy value—in this case Mc^2 —so the expression of Equation (14) needs to be divided by that before being used in Equations (4). An additional subtlety is that the modes β and γ also ought to have polar components of order ζ , which would thus couple to the axial components of the other two modes in the triplet (we will, however, neglect couplings of order ζ^2 and higher, involving the polar components of two or three modes). This means that we also need to evaluate $\kappa_{\bar{\beta}\gamma\bar{\alpha}}$ and $\kappa_{\bar{\gamma}\bar{\alpha}\beta}$, with the bar over the mode label meaning that the mode eigenfunction has to be complex conjugated in Equation (14). The complete expression for the coupling coefficient is then

$$\kappa = \frac{1}{Mc^2} (\kappa_{\alpha\beta\gamma} + \kappa_{\bar{\beta}\gamma\bar{\alpha}} + \kappa_{\bar{\gamma}\bar{\alpha}\beta}). \quad (16)$$

We will assume a background star with $M = 1.4 M_\odot$ (M_\odot being the solar mass) and $R_* = 10$ km, described by a polytropic equation of state $p \propto \rho^\Gamma$, with $\Gamma = 2$, for which the background quantities may be obtained analytically, and set the adiabatic exponent $\Gamma_1 = 2.1$ (see, for example, Andersson & Pnigouras 2020).

5. RESULTS

The coupled equations of motion (4) admit an analytical solution. Decomposing the complex mode amplitude Q_α into its real amplitude and phase components as

$$Q_\alpha = \frac{\varepsilon_\alpha e^{i\vartheta_\alpha}}{\kappa \sqrt{\omega_\beta \omega_\gamma}}, \quad (17)$$

Equations (4) become

$$\dot{\varepsilon}_\alpha = \varepsilon_\beta \varepsilon_\gamma \sin \varphi, \quad (18a)$$

$$\dot{\varepsilon}_\beta = -\varepsilon_\gamma \varepsilon_\alpha \sin \varphi, \quad (18b)$$

$$\dot{\varepsilon}_\gamma = -\varepsilon_\alpha \varepsilon_\beta \sin \varphi, \quad (18c)$$

and

$$\dot{\varphi} = \cos \varphi \left(\frac{\varepsilon_\beta \varepsilon_\gamma}{\varepsilon_\alpha} - \frac{\varepsilon_\gamma \varepsilon_\alpha}{\varepsilon_\beta} - \frac{\varepsilon_\alpha \varepsilon_\beta}{\varepsilon_\gamma} \right) + \Delta\omega, \quad (18d)$$

where $\varphi = \vartheta_\alpha - \vartheta_\beta - \vartheta_\gamma + \Delta\omega t$.

Including the phase ϑ_α in the harmonic time dependence of the mode we get $\xi_\alpha^i \propto e^{i(\omega_\alpha t + \vartheta_\alpha)}$, suggesting that the nonlinear coupling induces modulation of the mode frequency of the form $\omega'_\alpha = \omega_\alpha + \dot{\vartheta}_\alpha$, with the *shift* $\dot{\vartheta}_\alpha$ given by

$$\dot{\vartheta}_\alpha = \frac{\varepsilon_\beta \varepsilon_\gamma}{\varepsilon_\alpha} \cos \varphi. \quad (19)$$

Upon inspection, from the equations of motion (18) we can obtain the following constants of integration:

$$\mathcal{E}_1 = \varepsilon_\alpha^2 + \varepsilon_\beta^2, \quad (20)$$

$$\mathcal{E}_2 = \varepsilon_\alpha^2 + \varepsilon_\gamma^2, \quad (21)$$

and

$$L = \varepsilon_\alpha \varepsilon_\beta \varepsilon_\gamma \cos \varphi + \frac{\Delta\omega}{2} \varepsilon_\alpha^2, \quad (22)$$

with \mathcal{E}_1 and \mathcal{E}_2 being related to the energy of the mode triplet, whereas L dictates the evolution of the frequency shifts $\dot{\vartheta}_\alpha$. Combining Equations (18a) and (22), and making the replacement $\varepsilon_\alpha^2 = q\mathcal{E}_1$, we get

$$\left(\frac{dq}{dt} \right)^2 = 4\mathcal{E}_1 \left[q(1-q)(\mu-q) - \frac{1}{\mathcal{E}_1} \left(\frac{\Delta\omega}{2} q - \frac{L}{\mathcal{E}_1} \right)^2 \right], \quad (23)$$

with $\mu = \mathcal{E}_2/\mathcal{E}_1$. The expression in brackets on the right-hand side of Equation (23) is a cubic polynomial with roots q_1 , q_2 and q_3 , such that $q \in [q_1, q_2 \leq 1]$ and $q_3 \geq 1$.

We further replace $q = q_1 + (q_2 - q_1) \sin^2 \delta$, which makes Equation (23)

$$\left(\frac{d\delta}{dt} \right)^2 = \mathcal{E}_1 (q_3 - q_1) (1 - k^2 \sin^2 \delta), \quad (24)$$

with $k^2 = (q_2 - q_1)/(q_3 - q_1) \leq 1$. We integrate to get

$$\int_{\delta_0}^{\delta} \frac{d\delta'}{\sqrt{1 - k^2 \sin^2 \delta'}} = \sqrt{\mathcal{E}_1 (q_3 - q_1)} t, \quad (25)$$

from which we can define the *Jacobi elliptic function* $\text{sn}(u, k) = \sin \delta$ (e.g., Abramowitz & Stegun 1972), where

$$u(t) = \sqrt{\mathcal{E}_1 (q_3 - q_1)} t + \int_0^{\delta_0} \frac{d\delta}{\sqrt{1 - k^2 \sin^2 \delta}}, \quad (26)$$

with the angle δ_0 determined by the initial conditions for the mode amplitudes.

Switching to our initial variables, the solution to Equations (4) is

$$|Q_\alpha|^2 = \frac{\mathcal{E}_1}{\omega_\beta \omega_\gamma \kappa^2} [q_1 + (q_2 - q_1) \text{sn}^2(u, k)], \quad (27a)$$

$$|Q_\beta|^2 = \frac{\mathcal{E}_1}{\omega_\gamma \omega_\alpha \kappa^2} [1 - q_1 - (q_2 - q_1) \text{sn}^2(u, k)], \quad (27b)$$

$$|Q_\gamma|^2 = \frac{\mathcal{E}_1}{\omega_\alpha \omega_\beta \kappa^2} [\mu - q_1 - (q_2 - q_1) \text{sn}^2(u, k)]. \quad (27c)$$

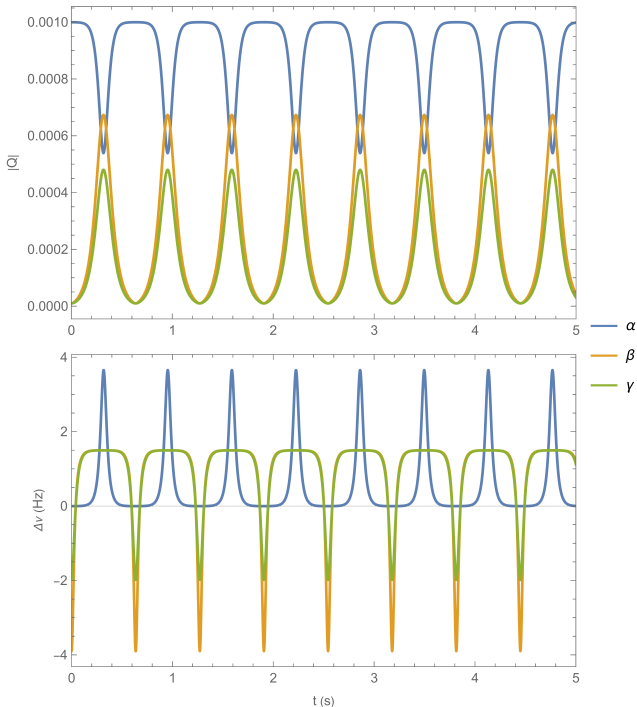


Figure 1. Evolution of our representative coupled mode triplet, with α labelling the high-frequency (parent) mode and β, γ the mid- and low-frequency (daughter) modes, respectively. We plot the mode amplitude $|Q|$ (*top*) and mode frequency shift $\Delta\nu \equiv \dot{\nu}/2\pi$ in Hz (*bottom*) as functions of time, for $\zeta = 4 \times 10^{-4}$ and initial conditions $|Q_\alpha| = 10^{-3}, |Q_\beta| = |Q_\gamma| = 10^{-5}$.

These are periodic with respect to time, with the period given by

$$T = \frac{2K(k)}{\sqrt{\mathcal{E}_1(q_3 - q_1)}}, \quad (28)$$

$K(k)$ being the *complete elliptic integral of the first kind*.

To demonstrate the system's behaviour, we will use the mode triplet of SGR 1900 [Equation (3)], with α labelling the high-frequency (*parent*) mode and β, γ the mid- and low-frequency (*daughter*) modes, respectively. The results are similar for the mode triplet in SGR 1806 [Equation (2)]. The initial mode amplitudes $|Q|$ are fixed, leaving ζ as the only free parameter.

In Fig. 1 we plot the evolution of the mode amplitudes $|Q|$ and frequency shifts $\Delta\nu \equiv \dot{\nu}/2\pi$ (in Hz) for $\zeta = 4 \times 10^{-4}$ and initial conditions $|Q_\alpha| = 10^{-3}, |Q_\beta| = |Q_\gamma| = 10^{-5}$. The energy exchange between the modes, characteristic for these systems, occurs periodically ($T \approx 0.7$ s), with the high-energy mode pumping energy into the low-energy modes, which then transfer it back, and the cycle repeats. Likewise, the frequency shift also oscillates periodically, with its maxima corresponding to minima in the amplitude and reaching values up to 4 Hz.

The period T of the amplitude modulation and the magnitude of the frequency shifts can be adjusted by changing ζ . Unless ζ falls below a certain limit value ζ_{lim} (see below), $(q_3 - q_1) \sim 1$ and $K(k) \sim 1$, so from Equation (28) we have $T \sim \mathcal{E}_1^{-1/2} \propto \kappa^{-1} \propto \zeta^{-1}$. The scaling of $\Delta\nu$ with ζ is more complicated. Expressing Equation (22) as $L = \varepsilon_\alpha^2(\dot{\nu}_\alpha + \Delta\omega/2)$ and noticing that $\varepsilon_\alpha^2 \dot{\nu}_\alpha = \varepsilon_\beta^2 \dot{\nu}_\beta = \varepsilon_\gamma^2 \dot{\nu}_\gamma$, one may derive the magnitudes of the frequency shifts as

$$\dot{\nu}_\alpha^{\text{mag}} = \frac{L}{\mathcal{E}_1} \frac{q_2 - q_1}{q_1 q_2}, \quad (29a)$$

$$\dot{\nu}_\beta^{\text{mag}} = \left(\frac{\Delta\omega}{2} - \frac{L}{\mathcal{E}_1} \right) \frac{q_2 - q_1}{(1 - q_1)(1 - q_2)}, \quad (29b)$$

$$\dot{\nu}_\gamma^{\text{mag}} = \left(\mu \frac{\Delta\omega}{2} - \frac{L}{\mathcal{E}_1} \right) \frac{q_2 - q_1}{(\mu - q_1)(\mu - q_2)}. \quad (29c)$$

These are increasing functions of ζ and approach zero in the linear limit, when $\zeta \approx \zeta_{\text{lim}}$ (or $q_1 \approx q_2$; see below). Hence, decreasing ζ leads both to larger modulation periods and smaller frequency shifts.

There is, however, a limit value, ζ_{lim} , to which we alluded earlier, below which the modes are too weakly coupled and their amplitudes are practically constant (essentially, the system approaches the linear limit). This occurs when $q_1 \approx q_2$, or when the discriminant of the cubic polynomial in q from Equation (23) gets close to zero. The value of ζ_{lim} depends on the value of the detuning $\Delta\omega$: the larger $\Delta\omega$ is, the larger ζ_{lim} is. This is sensible, because a small detuning implies a stronger nonlinear resonance and, hence, stronger nonlinear coupling among the three modes [see Equation (10)], which allows for smaller values of the coupling coefficient.

For the triplet we are examining, the case depicted in Fig. 1 is already near ζ_{lim} . In order to explain the appearance and disappearance of modes over timescales of order 10 – 100 s, which is what QPO observations suggest, we need lower values of ζ . Let us, therefore, reduce the original value of the detuning ($\Delta\omega/2\pi = 3$ Hz) by a factor of 1000. For this case, we plot $|Q|$ and $\Delta\nu$ in Fig. 2 for three different values of ζ and using the same initial conditions as before, in order to demonstrate that the variation of ζ affects T and $\Delta\nu$ according to the scalings presented before. In particular, for $\zeta = 5 \times 10^{-6}$ we obtain $T \approx 50$ s and $\Delta\nu_\alpha$ reaches values up to 1 Hz; for $\zeta = 10^{-5}$ the period drops to $T \approx 25$ s and $\Delta\nu_\alpha$ increases to up to 3 Hz; and for $\zeta = 3 \times 10^{-5}$ the period is $T \approx 9$ s, with $\Delta\nu_\alpha$ getting up to 30 Hz.

Moreover, in Fig. 3 we plot $|Q|$ and $\Delta\nu$ for the same parameters as in the first column of Fig. 2, but also assuming an amplitude detection cutoff, set to $|Q| = 4 \times 10^{-4}$. When the amplitude becomes lower than this cutoff value, the mode is regarded as undetectable, and its amplitude and frequency shift curves are plotted as semi-transparent. This way we mimic the observed appearance and disappearance of modes in giant flare tails.

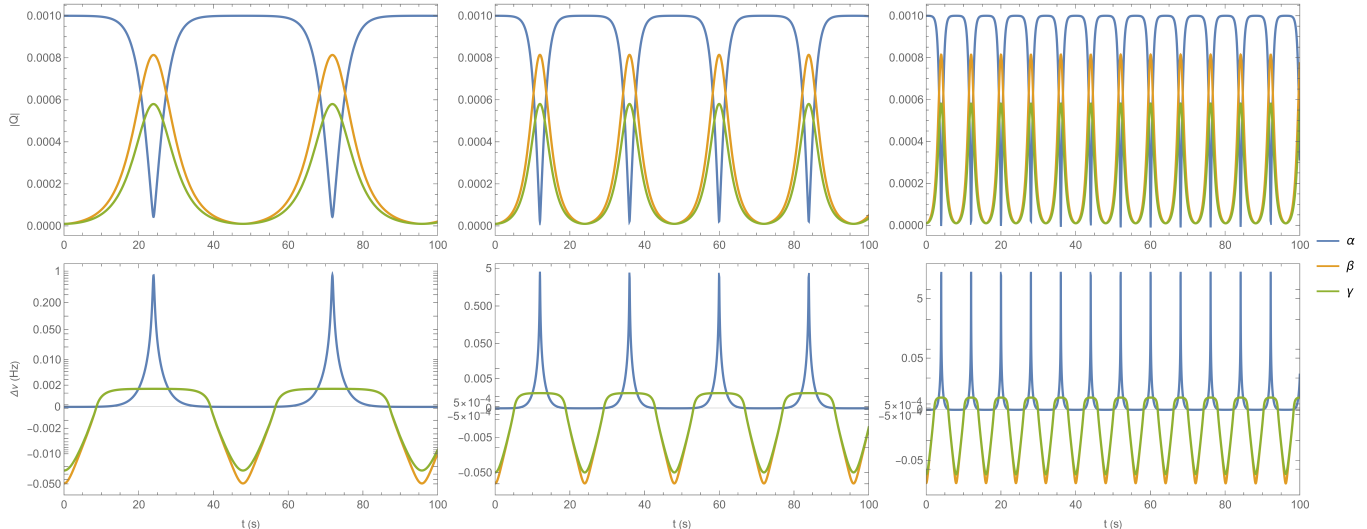


Figure 2. The effect of varying ζ on $|Q|$ (*top panels*) and $\Delta\nu$ (*bottom panels*), for the same initial conditions as for Fig. 1, but with the detuning dropped by a factor of 1000. From left to right: $\zeta = 5 \times 10^{-6}$, 10^{-5} , 3×10^{-5} .

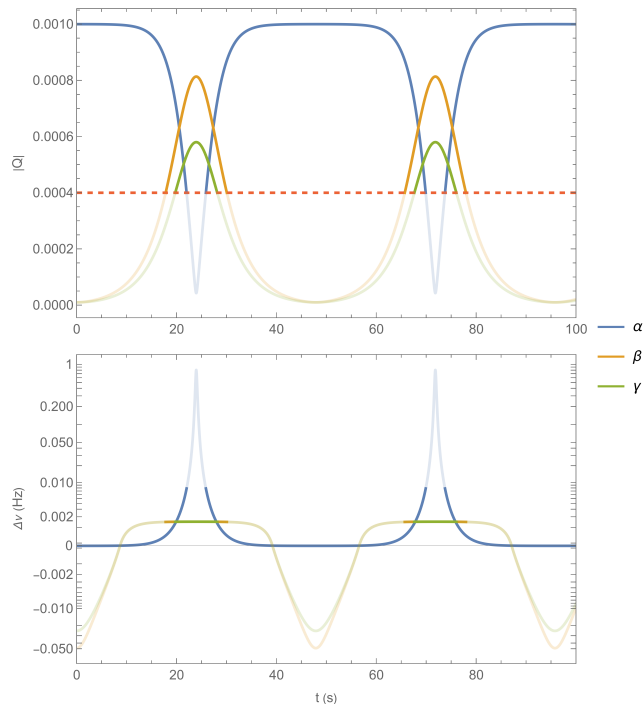


Figure 3. Evolution of $|Q|$ and $\Delta\nu$ from the first column of Fig. 2, but now assuming an amplitude detection cutoff $|Q| = 4 \times 10^{-4}$ (*dashed line*).

Finally, note that our choice of initial conditions is such that $\zeta_{\text{lim}} \ll 1$. Increasing the initial mode amplitudes practically has the same effect as increasing ζ (and vice versa), which is to be expected; a large mode amplitude would imply that we are deep into the nonlinear regime, hence the coupling coefficient (parametrised by ζ) need not be as large for the characteristic energy exchange to occur among the three modes.

6. DISCUSSION

The apparent disappearance and reappearance of magnetar QPOs, together with their drifting frequencies, are important observations that have previously received little attention from theoretical modelling [a rare exception being the work of Levin (2007)]. We have found that both phenomena can be explained through nonlinear mode coupling. In such a system, mode amplitudes have oscillatory variation in time (rather than simply decaying), and also time-varying frequency shifts, providing a concrete physical reason to believe that, e.g., the 26-Hz and 30-Hz QPOs of SGR 1806 are the same oscillation mode.

There is one key free parameter ζ in our coupled mode triplet, which quantifies the strength of the subdominant polar piece of a predominantly axial mode. This is required, because the most readily excited magnetar modes are axial, but three purely axial modes do not experience any coupling. The value of ζ dictates the timescale on which a given mode dis-/re-appears, and also its drift in frequency. We argue that it is natural to associate ζ with the toroidal component of the star's magnetic field; the behaviour of a magnetar's QPOs could thus be one of very few possible mechanisms for inferring the star's internal field geometry.

Although we can mimic QPO dis-/re-appearance over the observed timescales, or observed shifts in frequency of some QPOs, it is more challenging to get both right with our simple coupled-triplet model – partly because we predict the maximum frequency shift to occur when the mode is least likely to be detectable. Furthermore, the real data does not indicate that QPO variability is strictly periodic, as our model predicts. It is, however, easy to see where further complexity could come from in the mode coupling, perhaps resulting in better agreement with observations. Firstly, the fact that

the $\sim 57, \sim 90, \sim 150$ -Hz QPOs are also likely to couple together (based on the frequency selection rule, i.e. $57 + 90 \approx 150$) – involving two of the same modes as our fiducial triplet here – suggests a possible coupling between the two *triplets* . Further complexity would come if we allowed for energy to be dissipated from the modes (rather than just transferred between them). Finally, we need to recall that we do not observe these QPOs directly, as oscillations of the star’s surface, but rather as modulations to the brightness of a fireball anchored to the star by magnetic field lines (Gabler et al. 2014; Akgün et al. 2018). This process will affect how ‘visible’ certain modes are, on top of the intrinsic changes in amplitude that mode coupling gives.

Higher-frequency QPOs ($\gtrsim 600$ Hz) are more likely to represent non-axisymmetric modes, whose eigenfunctions would be sufficiently different as to inhibit coupling with axisymmetric mode triplets like those we focus on here. In the tail following the giant flare of SGR 1806, these high-frequency QPOs exhibited similar behaviour to the lower-frequency QPOs (Watts & Strohmayer 2006), suggesting a process of mode coupling in this case

too. Intriguingly, high-frequency QPOs were also seen *during* the giant flare from an extragalactic magnetar (Castro-Tirado et al. 2021), suggesting that these may be preferentially excited during the initial phase, and perhaps couple to other modes much later on.

PP acknowledges support from the María Zambrano Fellowship Programme (ZAMBRANO21-22), funded by the Spanish Ministry of Universities and the University of Alicante through the European Union’s “Next Generation EU” package, as well as from the grant PID2021-127495NB-I00, funded by MCIN/AEI/10.13039/501100011033 and by the European Union, from the Astrophysics and High Energy Physics programme of the Generalitat Valenciana ASFAE/2022/026, funded by the Spanish Ministry of Science and Innovation (MCIN) and the European Union’s “Next Generation EU” package (PRTR-C17.I1), and from the Prometeo 2023 excellence programme grant CIPROM/2022/13, funded by the Ministry of Education, Culture, Universities, and Occupation of the Generalitat Valenciana.

REFERENCES

- Abramowitz, M., & Stegun, I. A. 1972, Handbook of Mathematical Functions (New York: Dover).
<http://adsabs.harvard.edu/abs/1972hmfw.book....A>
- Akgün, T., Cerdá-Durán, P., Miralles, J. A., & Pons, J. A. 2018, MNRAS, 481, 5331, doi: [10.1093/mnras/sty2669](https://doi.org/10.1093/mnras/sty2669)
- Andersson, N., & Pnigouras, P. 2020, PhRvD, 101, 083001, doi: [10.1103/PhysRevD.101.083001](https://doi.org/10.1103/PhysRevD.101.083001)
- Arras, P., Flanagan, É. É., Morsink, S. M., et al. 2003, ApJ, 591, 1129, doi: [10.1086/374657](https://doi.org/10.1086/374657)
- Castro-Tirado, A. J., Østgaard, N., Göğüş, E., et al. 2021, Nature, 600, 621, doi: [10.1038/s41586-021-04101-1](https://doi.org/10.1038/s41586-021-04101-1)
- Cerdá-Durán, P., Stergioulas, N., & Font, J. A. 2009, MNRAS, 397, 1607, doi: [10.1111/j.1365-2966.2009.15056.x](https://doi.org/10.1111/j.1365-2966.2009.15056.x)
- Colaiuda, A., & Kokkotas, K. D. 2012, MNRAS, 423, 811, doi: [10.1111/j.1365-2966.2012.20919.x](https://doi.org/10.1111/j.1365-2966.2012.20919.x)
- Duncan, R. C. 1998, ApJL, 498, L45, doi: [10.1086/311303](https://doi.org/10.1086/311303)
- Dziembowski, W. 1982, Acta Astron., 32, 147.
<http://adsabs.harvard.edu/abs/1982AcA....32..147D>
- Gabler, M., Cerdá-Durán, P., Stergioulas, N., Font, J. A., & Müller, E. 2013, PhRvL, 111, 211102, doi: [10.1103/PhysRevLett.111.211102](https://doi.org/10.1103/PhysRevLett.111.211102)
- . 2014, MNRAS, 443, 1416, doi: [10.1093/mnras/stu1263](https://doi.org/10.1093/mnras/stu1263)
- . 2016, MNRAS, 460, 4242, doi: [10.1093/mnras/stw1272](https://doi.org/10.1093/mnras/stw1272)
- Hambaryan, V., Neuhäuser, R., & Kokkotas, K. D. 2011, A&A, 528, A45, doi: [10.1051/0004-6361/201015273](https://doi.org/10.1051/0004-6361/201015273)
- Huppenkothen, D., Heil, L. M., Watts, A. L., & Göğüş, E. 2014, ApJ, 795, 114, doi: [10.1088/0004-637X/795/2/114](https://doi.org/10.1088/0004-637X/795/2/114)
- Israel, G. L., Belloni, T., Stella, L., et al. 2005, ApJL, 628, L53, doi: [10.1086/432615](https://doi.org/10.1086/432615)
- Kouveliotou, C., Dieters, S., Strohmayer, T., et al. 1998, Nature, 393, 235, doi: [10.1038/30410](https://doi.org/10.1038/30410)
- Lee, U. 2008, MNRAS, 385, 2069, doi: [10.1111/j.1365-2966.2008.12965.x](https://doi.org/10.1111/j.1365-2966.2008.12965.x)
- Levin, Y. 2007, MNRAS, 377, 159, doi: [10.1111/j.1365-2966.2007.11582.x](https://doi.org/10.1111/j.1365-2966.2007.11582.x)
- Markey, P., & Tayler, R. J. 1973, MNRAS, 163, 77, doi: [10.1093/mnras/163.1.77](https://doi.org/10.1093/mnras/163.1.77)
- Mereghetti, S., Esposito, P., Tiengo, A., et al. 2006, ApJ, 653, 1423, doi: [10.1086/508682](https://doi.org/10.1086/508682)
- Miller, M. C., Chirenti, C., & Strohmayer, T. E. 2019, ApJ, 871, 95, doi: [10.3847/1538-4357/aaf5ce](https://doi.org/10.3847/1538-4357/aaf5ce)
- Nayfeh, A. H., & Mook, D. T. 1979, Nonlinear Oscillations (New York: John Wiley & Sons).
<http://adsabs.harvard.edu/abs/1979noos.book....N>
- Palmer, D. M., Barthelmy, S., Gehrels, N., et al. 2005, Nature, 434, 1107, doi: [10.1038/nature03525](https://doi.org/10.1038/nature03525)
- Passamonti, A., & Lander, S. K. 2013, MNRAS, 429, 767, doi: [10.1093/mnras/sts372](https://doi.org/10.1093/mnras/sts372)
- . 2014, MNRAS, 438, 156, doi: [10.1093/mnras/stt2134](https://doi.org/10.1093/mnras/stt2134)
- Pnigouras, P., & Kokkotas, K. D. 2015, PhRvD, 92, 084018, doi: [10.1103/PhysRevD.92.084018](https://doi.org/10.1103/PhysRevD.92.084018)

- . 2016, *PhRvD*, 94, 024053,
doi: [10.1103/PhysRevD.94.024053](https://doi.org/10.1103/PhysRevD.94.024053)
- Pumpe, D., Gabler, M., Steininger, T., & Enßlin, T. A. 2018, *A&A*, 610, A61, doi: [10.1051/0004-6361/201731800](https://doi.org/10.1051/0004-6361/201731800)
- Roberts, O. J., Baring, M. G., Huppenkothen, D., et al. 2023, *ApJL*, 956, L27, doi: [10.3847/2041-8213/acfcad](https://doi.org/10.3847/2041-8213/acfcad)
- Sakurai, J. J., & Napolitano, J. 2011, *Modern Quantum Mechanics*, 2nd edn. (San Francisco: Addison-Wesley).
<http://adsabs.harvard.edu/abs/1985mqm..book.....S>
- Samuelsson, L., & Andersson, N. 2007, *MNRAS*, 374, 256,
doi: [10.1111/j.1365-2966.2006.11147.x](https://doi.org/10.1111/j.1365-2966.2006.11147.x)
- Schenk, A. K., Arras, P., Flanagan, É. É., Teukolsky, S. A., & Wasserman, I. 2001, *PhRvD*, 65, 024001,
doi: [10.1103/PhysRevD.65.024001](https://doi.org/10.1103/PhysRevD.65.024001)
- Sotani, H., Kokkotas, K. D., & Stergioulas, N. 2007, *MNRAS*, 375, 261, doi: [10.1111/j.1365-2966.2006.11304.x](https://doi.org/10.1111/j.1365-2966.2006.11304.x)
- Steiner, A. W., & Watts, A. L. 2009, *PhRvL*, 103, 181101,
doi: [10.1103/PhysRevLett.103.181101](https://doi.org/10.1103/PhysRevLett.103.181101)
- Strohmayer, T. E., & Watts, A. L. 2005, *ApJ*, 632, L111,
doi: [10.1086/497911](https://doi.org/10.1086/497911)
- . 2006, *ApJ*, 653, 593, doi: [10.1086/508703](https://doi.org/10.1086/508703)
- Unno, W., Osaki, Y., Ando, H., Saio, H., & Shibahashi, H. 1989, *Nonradial Oscillations of Stars*, 2nd edn. (Tokyo: University of Tokyo Press).
<http://adsabs.harvard.edu/abs/1989nos..book.....U>
- van Hoven, M., & Levin, Y. 2012, *MNRAS*, 420, 3035,
doi: [10.1111/j.1365-2966.2011.20177.x](https://doi.org/10.1111/j.1365-2966.2011.20177.x)
- Watts, A. L., & Strohmayer, T. E. 2006, *ApJL*, 637, L117,
doi: [10.1086/500735](https://doi.org/10.1086/500735)
- Weinberg, N. N., Arras, P., & Burkart, J. 2013, *ApJ*, 769, 121, doi: [10.1088/0004-637X/769/2/121](https://doi.org/10.1088/0004-637X/769/2/121)
- Weinberg, N. N., Arras, P., Quataert, E., & Burkart, J. 2012, *ApJ*, 751, 136, doi: [10.1088/0004-637X/751/2/136](https://doi.org/10.1088/0004-637X/751/2/136)
- Wright, G. A. E. 1973, *MNRAS*, 162, 339,
doi: [10.1093/mnras/162.4.339](https://doi.org/10.1093/mnras/162.4.339)
- Wu, Y., & Goldreich, P. 2001, *ApJ*, 546, 469,
doi: [10.1086/318234](https://doi.org/10.1086/318234)
- Younes, G., Baring, M. G., Kouveliotou, C., et al. 2017, *ApJ*, 851, 17, doi: [10.3847/1538-4357/aa96fd](https://doi.org/10.3847/1538-4357/aa96fd)